

The emplacement of low-aspect ratio ignimbrites by turbulent parent flows

W. B. Dade¹

Institute of Theoretical Geophysics, University of Cambridge, Cambridge, UK

Received 20 August 2001; revised 6 September 2002; accepted 30 September 2002; published 19 April 2003.

[1] A quantitative model for a radially spreading, suspension-driven gravity current is used to interpret parent flow conditions of a volumetrically wide range of pyroclastic deposits known from the recent and ancient geologic records of explosive volcanism. The analysis, which requires no freely adjustable parameters, yields values of the solids concentration, time of duration (or, equivalently, a minimal estimate of eruptive flux of solids) and average speed for the ground-hugging, deposit-forming gravity currents. A consistent picture emerges in which the initial volumetric concentration of pyroclastic solids in the parent flows is of the order 10^{-2} or less, and the expanded flows travel with average speeds in the range $25\text{--}250\text{ m s}^{-1}$ to reach their farthest extent in a matter of only minutes. Further application of the model suggests that depositional structures in a widespread and thin ignimbrite are likely to reflect the intensity of mass flux in the parent flow, and thus the intensity and overall volume of the parent eruption. Conditions in small-magnitude pyroclastic currents of recent history can result in cross-stratified deposits. Primary sedimentary structures (or their absence) in some regionally widespread and massive deposits known only in the geologic record, in contrast, were probably emplaced under conditions of intense sheet-flow transport driven by the parent gravity

currents. **INDEX TERMS:** 8404 Volcanology: Ash deposits; 8414 Volcanology: Eruption mechanisms; 8499 Volcanology: General or miscellaneous; **KEYWORDS:** Pyroclastic flow, ignimbrite, volcanoclastic deposit

Citation: Dade, W. B., The emplacement of low-aspect ratio ignimbrites by turbulent parent flows, *J. Geophys. Res.*, 108(B4), 2211, doi:10.1029/2001JB001010, 2003.

1. Introduction

[2] An explosive volcanic eruption can, under certain conditions, result in a rapidly moving, ground-hugging flow of hot gas, pumice and ash. The poorly sorted and pumice-rich deposit, for which average component particle size is typically of order 1 mm, is called an ignimbrite or ash-flow tuff. Many such deposits, such as those emplaced during the eruptions of Katmai in 1912, Mount Pinutubo in 1991, and Soufriere Hills Volcano on Montserrat during October 1997, are relatively thick and are confined to topographically bounded valleys and plains. In the largest and most violent ignimbrite-forming events, currently known only from the geologic record, the parent flow is extremely mobile and generates a radially symmetric deposit that thinly mantles the preexisting landscape [Walker *et al.*, 1980]. The aspect ratio AR of such a deposit, defined as the ratio of its average thickness to the radius of a circle of equal area in plan, is of the order of 10^{-4} or less (Figure 1; Table 1). Thus, such a deposit is often referred to as a low-aspect ratio ignimbrite, or LARI. On the basis of geometrical similarity alone, the

pyroclastic currents and deposits generated by the relatively small magnitude eruptions of El Chichón in 1982, during which 2000 people perished, serve as small-scale examples of LARI phenomena [Sigurdsson *et al.*, 1984, 1987a, 1987b]. This perspective is not universally accepted by volcanologists, and exploring its validity is the purpose of this paper.

[3] The issues involved are of timely significance. The hazards associated with relatively small but frequent events, such as occurred at Mount St. Helens in 1980 or at El Chichón, are severe enough. Similar types of events involving extremely large eruptive volumes near a population center would be commensurately disastrous. Accordingly, reconstruction of the parent flows of ancient, large-volume ignimbrites with low-aspect ratio is an important part of ongoing studies of the hazards of explosive volcanism [Gilbert and Sparks, 1998].

[4] In the following section, two perspectives regarding the mechanism of emplacement of regionally widespread ignimbrites with low-aspect ratio are discussed. This review is not exhaustive, but serves rather to introduce a larger, ongoing debate. The key elements of a model for one end-member scenario in this debate, that of a radially spreading, turbulent suspension-driven gravity current, are then briefly reviewed. This model is used to infer representative conditions in the parent flows of selected pyroclastic deposits of low-aspect ratio. The results of the analysis are then

¹Now at Department of Earth Sciences, Dartmouth College, Hanover, New Hampshire, USA.

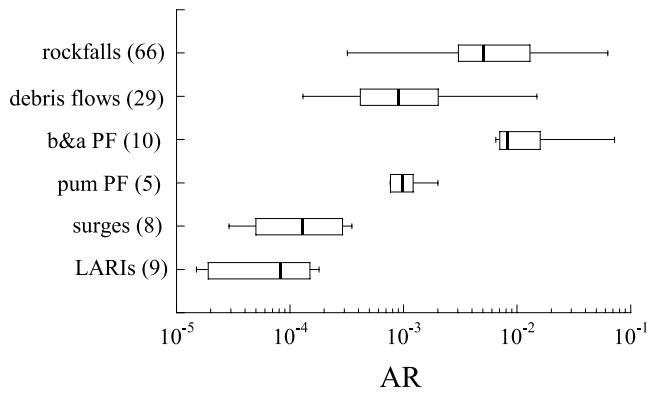


Figure 1. Box and whisker plots of observed values of the aspect ratio AR of the pyroclastic deposits listed in Table 1, deposits recently emplaced by densely concentrated, small-volume pyroclastic flows of pumice and ash (Pum PF) and block and ash (B&A PF) on Montserrat, and deposits emplaced by noneruptive debris flows and lahars, and dry rockfalls and avalanches on the Earth, Moon, and Mars. The values in parentheses indicate the number of observations in each class of deposit. The heavy vertical line of each box plot indicates the median value for each of class of deposit, the box indicates the central two quartiles, and the horizontal lines indicate the range of the extreme values. Data from the references listed in Table 1, *Iverson et al.* [1998], and *Dade and Huppert* [1998] and original references therein.

extended to provide new insight into the possible factors that control the internal structure of these deposits.

[5] In a larger sense, the aim of this study is to demonstrate how a simple, physics-based model can be used to interpret some pyroclastic deposits known only from the

geologic record, and to identify new issues which should be considered in the ongoing debate regarding the mechanisms and associated hazards of LARI emplacement. The approach developed here is thus complementary to more detailed, numerical treatments of ash-flow dynamics undertaken by, for example, *Bursik and Woods* [1996].

2. Turbulent Beginnings

[6] A thorough review of the dynamics and deposits of pyroclastic gravity currents can be found in, for example, *Druitt* [1998]. Here, a few ideas are briefly discussed to introduce key concerns.

[7] The geologic record of explosive volcanism is currently viewed from two perspectives. By analogy with the basal surge associated with a collapsing plume generated by a nuclear explosion, *Fisher* [1966] proposed that the parent flow of a pyroclastic deposit that is widespread and thin, and therefore of low-aspect ratio, is a highly expanded, turbulent gravity current that propagates radially from the base of a collapsing eruption column. As the ground-hugging flow rolls over the existing terrain, it leaves a veneer of pumice and ash which accumulates progressively from the fallout of suspended material. This view of LARI emplacement is consistent with the extreme mobility of some parent flows over the sea and over 1-km high topography [*Aramaki and Ui*, 1966; *Fisher et al.*, 1993] as well as the observed degree of size- and compositional-sorting of material in the transport direction [*Druitt*, 1992; *Dade and Huppert*, 1996]. Dune-like bedforms and cross stratification preserved in deposits associated with recent, relatively small magnitude eruptions are taken to indicate the dilute and turbulent nature of some pyroclastic gravity currents, including, for example, those generated during the eruption of El Chichón [*Moore*, 1967; *Sigurdsson et al.*, 1984, 1987a, 1987b; *Druitt*, 1992]. Potentially important exten-

Table 1. Observed Properties of Pyroclastic Surge Deposits and LARIs, and Inferred Properties of Their Parent Eruptions and Flows^a

	V_s , (km ³)	A_s , km ²	L , km	λ	AR_s , $\times 10^{-4}$	C_o , $\times 10^{-2}$	T , s	Q_s , m ³ s ⁻¹	U_{av} , m s ⁻¹	L_o , km	Yield, J	Θ	References
<i>Surge Deposits</i>													
Montserrat 6/97	0.0008	4	6.7	0.1	3.5	0.4	191	4×10^3	35	0.4	3×10^{11}	0.5	<i>Calder et al.</i> [1999]
Montserrat 12/97	0.0025	9.8	5	0.4	2.9	0.7	127	2×10^4	40	0.5	1×10^{13}	0.6	<i>Calder et al.</i> [1999]
Taal	0.0050	50	4	π	0.5	0.2	162	3×10^4	25	0.8	4×10^{13}	0.3	<i>Waters and Fisher</i> [1971]
El Chichón S1	0.0325	93	6	π	1.3	0.9	130	3×10^5	46	1	3×10^{14}	0.9	<i>Sigurdsson et al.</i> [1987a, 1987b]
El Chichón S2	0.0450	104	6	π	1.5	1.2	117	4×10^5	52	1	4×10^{14}	1.1	<i>Sigurdsson et al.</i> [1987a, 1987b]
Lamington	0.1	200	8	π	1.3	1.1	145	7×10^5	55	1.3	1×10^{15}	1.3	<i>Francis</i> [1993]; <i>Simkin and Seibert</i> [1994]
Mt. Saint Helens	0.1	527	20	1.3	0.3	0.1	587	2×10^5	34	2.8	3×10^{15}	0.5	<i>Moore and Sisson</i> [1983]
Rabaul	0.6	1200	20	3	0.5	0.5	360	2×10^6	55	3.2	2×10^{16}	1.3	<i>Walker</i> , 1983; <i>McKee et al.</i> [1985]
<i>LARIs</i>													
Vulsini B	1.8	1250	20	π	1.4	2.1	216	8×10^6	93	2.7	5×10^{16}	3.5	<i>Sparks</i> [1975]
Koya	5	11000	60	3	0.2	0.1	1137	4×10^6	53	10	5×10^{17}	1.1	<i>Walker et al.</i> [1980]
Tosu	5	10000	100	1	0.2	0.1	1807	3×10^6	55	11	5×10^{17}	1.3	<i>Susuki-Kamata and Kamata</i> [1990]
Taupo	15	20000	80	π	0.2	0.2	1180	1×10^7	68	12	2×10^{18}	1.9	<i>Wilson</i> [1985]
Guatamala H	18	16000	125	1	0.3	0.2	1506	1×10^7	83	12	2×10^{18}	2.8	<i>Koch and McLean</i> [1975]
Ito	50	15000	70	3	1	2.2	490	1×10^8	143	8	4×10^{18}	8.3	<i>Walker et al.</i> [1980]
Kidnappers	225	45000	120	π	0.8	2.4	686	3×10^8	175	13	3×10^{19}	12.5	<i>Wilson et al.</i> [1995]
Campanian	250	31400	100	π	1.6	5.7	453	6×10^8	220	10	3×10^{19}	19.9	<i>Fisher et al.</i> [1993]
Rattlesnake	330	35000	120	2.4	1.8	6.1	499	7×10^8	240	11	4×10^{19}	23.6	<i>Streck and Grunder</i> [1995]

^aSymbols as defined in the text and Table 2. Estimates of solids volume V_s , inundated area A and inferred eruptive flux Q represent minimal values. In considering the estimated explosive yield of parent eruptions, note that a one kiloton nuclear device has a nominal yield of 4.2×10^{12} J, and the amount of energy consumed globally each year is currently in excess of 3×10^{20} J.

sions of this view accommodate (1) the effects of density stratification in the particle suspension that drives the parent flow [Valentine, 1987; Valentine and Wohletz, 1989], (2) the effects of the entrainment of ambient air by parent flows [Bursik and Woods, 1996], (3) far-reaching bedload transport of very large particles by a suspension-driven flow [Dade and Huppert, 1996], (4) the reversal of buoyancy and the attendant development of coignimbrite phenomena [e.g., Dade and Huppert, 1995; Bursik and Woods, 1996; Druitt, 1998], and (5) the potential for local syn- and immediately postemplacement draining of material into topographic lows in the form of relatively small-volume granular flows and avalanches [Fisher, 1990; Druitt, 1992; Calder et al., 1999].

[8] In contrast, Sparks et al. [1976, 1978] proposed that most ignimbrites, including ancient, large volume deposits of low-aspect ratio, are emplaced en masse by parent flows that are nonturbulent and avalanche-like. The presence of overpressured gasses generated by exsolution from component juvenile particles, volatilization of surface moisture and ingestion of ambient air at the flow front make secondary but nevertheless potentially important contributions to the enhanced mobility of the flow. The dense-flow model has gained wide acceptance in the analysis of ancient, large volume ignimbrites [e.g., Wilson, 1980a, 1980b, 1985] and has become an essential component of textbook discussions of such deposits [e.g., Francis, 1993]. Among the observations offered in support of dense-flow emplacement of LARIs are thick, ponded deposits and rafts of pumice boulders in topographic lows [Wilson, 1985; Wilson et al., 1997]. Also cited as evidence in favor of dense parent flows of ancient, large-volume ignimbrites are a general absence of well-developed bedforms and internal cross stratification, in contrast with features observed in the small-volume deposits mentioned above. Ancient, large-volume LARIs instead comprise massive, featureless bedding, crude laminations and inverse grading.

[9] The view that LARIs are universally emplaced by dense flows has come under renewed scrutiny [Valentine and Fisher, 1993]. Branney and Kokelaar [1992], for example, have raised important questions about the significance of the depositional features that are often observed in pyroclastic deposits, and have offered alternative interpretations. Ponded deposits and related features are now recognized as potential products of highly condensed, late-stage flows that are subject to local topographic control [Fisher, 1990; Druitt, 1992, 1998; Dade and Huppert, 1996; Wilson et al., 1997]. Observations of such phenomena associated with the recent eruptions of Mount Pinutubo [Torres et al., 1997] and the Soufriere Hills Volcano [Calder et al., 1999] reinforce this view. The significance of the primary sedimentary structures observed in recent, small-volume surge deposits and ancient, large-volume LARIs is revisited later in this analysis.

[10] A useful starting point for quantitatively constraining the runout behavior of a densely concentrated pyroclastic flow is a comparison with noneruptive yet highly mobile rockfalls and debris flows. Hayashi and Self [1992], for example, empirically observed that the mobilities of many pyroclastic flows that resulted in ignimbrites of relatively high aspect ratio are not significantly different from the mobilities of dry, long-runout avalanches of noneruptive origin. This view is reinforced here when the comparison is

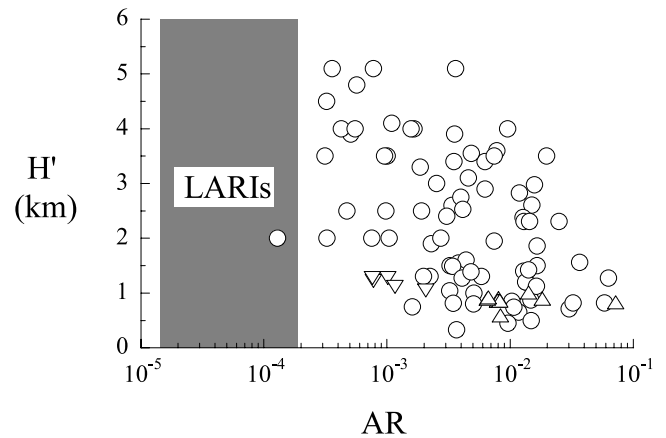


Figure 2. Aspect ratio AR as a function of nominal height of fall H' for dense flows of noneruptive origin on the Earth, Moon, and Mars, and dense pyroclastic flows generated during the recent eruption of Soufriere Hills Volcano, Montserrat. All heights of fall have been adjusted to correspond to equivalent terrestrial potential elevations. Open circles represent observations of noneruptive flows, triangles represent block and ash flows on Montserrat, and inverted triangles represent pumiceous pyroclastic flows on Montserrat. For comparison, the range of AR values of ancient LARIs is indicated by shading. Data as in Figure 1.

made in terms of the aspect ratios of the respective types of mass-flow deposits, including those of dense pyroclastic gravity currents on Montserrat (Figure 1).

[11] A further comparison can be pursued as follows. In a recent analysis of noneruptive avalanches and related phenomena, Dade and Huppert [1998] considered a mass of debris of bulk density ρ that falls from a height H and is subjected to a constant, resisting shear stress τ during runout. The predicted aspect ratio AR of the resulting debris deposit is proportional to $\tau/\rho gH$, where g is the acceleration of gravity and the implicit, dimensionless coefficient of proportionality is related to the angular distribution of deposit in plan. Thus, the wide range in observed values of the aspect ratio of noneruptive rockfalls and debris flows indicated in Figure 1 is in part owing to the range of known heights of fall, with greater heights resulting in potentially smaller values of AR (Figure 2). The additional, significant scatter in the observations reflects differences in site-specific, geological factors. These include differences in the composition of the debris, the presence of varying amounts of pore fluids, and local topographic control of the paths of runout.

[12] If densely concentrated pyroclastic flows are analogous to noneruptive avalanches and related mass flows, then very small values of deposit aspect ratio AR require relatively low resisting stress or a very large height of fall. Values of τ very much less than those observed for noneruptive mass flows would suggest that new perspectives on the dynamics of densely concentrated pyroclastic mass flows are required. Such a shift in perspectives does not, however, seem to be warranted given the comparable cross-sectional geometries of, say, deposits emplaced by pumiceous pyroclastic flows on Montserrat and by water-fluidized, and therefore relatively mobile, noneruptive

debris flows (Figure 1). On the other hand, a crude extrapolation of the observations of noneruptive, densely concentrated flow phenomena shown in Figure 2 implies that a fall of debris from a height of several km or more would be required for the resulting deposit to exhibit an aspect ratio that approaches 10^{-4} . While this constraint is not unreasonable for an extremely explosive eruption, it is worth noting that the ascent of, say, 10 km^3 of volcanic ejecta to a height of 10 km requires approximately 10^{18} J. This amount of energy readily exceeds the yield of the single largest thermonuclear device ever detonated. If such amounts of energy were to be rapidly unleashed in an explosive eruption, one could expect with certainty a volcanogenic fireball that is highly expanded and turbulent. The explosive distribution of a smaller volume of ash to a similar elevation would require proportionally less energy, but would also result in an eruption cloud which is, on average, even more dilute.

[13] Upon explosive emplacement, a volcanic eruption cloud that is dilute but nevertheless sufficiently laden with ash will be denser than the surrounding atmosphere. This condition is favored by low water content of the source magma and a relatively large volcanic vent [Druitt, 1998; Woods, 1998]. As a result of its relative density, the eruption cloud will immediately proceed to spread under the influence of gravity as a highly turbulent and ground-hugging ash flow and will simultaneously lose its driving, excess density owing to particle fallout. This scenario is now examined in greater detail.

3. Application of an Existing Model for an Axisymmetric, Suspension-Driven Gravity Current

[14] Dade and Huppert [1995] considered the vertically averaged equations that govern the evolution of a suspension-driven gravity current that spreads radially from a source and progressively loses, owing to particle fallout, the driving force associated with its excess density. Source conditions of either instantaneous volume release or constant flux were accommodated in the original analysis. A conventional Froude number condition serves as a surrogate momentum equation in the model, and the rate of particle fallout is related to the product of settling speed and solids concentration. The Froude number is a dimensionless ratio of flow speed and the root product of effective gravity and flow depth and, for inertial gravity currents over laboratory surfaces of negligible slope, takes on a value very close to unity [e.g., Simpson, 1987]. In the case of a current generated by the instantaneous release of a dense suspension, a simple geometric argument that relates flow volume, thickness and radial travel distance provides the necessary closure for the coupled equations. Here, we review only the key results of the model developed by Dade and Huppert [1995].

[15] The model assumptions relevant here are that the relatively dilute flow propagates over terrain with low relative relief and small regional slope, and that the ratio of the characteristic fall speed of component ejecta particles w_s to flow speed U_{av} be much less than unity. For the sake of explicitness, this last point is stated mathematically as

$$\beta \ll w_s/U_{av} \ll 1, \quad (1)$$

Table 2. Characteristic Scales of Length, Area and Time of Emplacement by a Turbulent, Axisymmetric Gravity Current Driven by a Deposit-Forming Suspension of Fine Particles^a

Runout Length, L	Inundated Area, A	Time of Duration, T
$L = \left(\frac{64F^2}{\lambda^3}\right)^{1/8} \left\{ \frac{\gamma g V_s^3}{(w_s C_0)^2} \right\}^{1/8}$	$A = (64F^2)^{1/4} \left\{ \frac{g \gamma \lambda V_s^3}{(w_s C_0)^2} \right\}^{1/4}$	$T = \left(\frac{4\lambda L^4}{F^2 \gamma g V_s}\right)^{1/2}$

^a g is acceleration due to gravity; V_s and C_0 are initial volume and concentration of solids in a parent flow; w_s and γ are the characteristic fall speed and dimensionless, relative excess density of individual particles in the flow; F is Froude number of the parent flow (assumed in this analysis to be unity); and $\lambda \equiv A/L^2$ is the geometric aspect of the deposit in plan. Expressions are modified from Dade and Huppert [1995].

where β is the regional slope of the inundated landscape in radians. Under these conditions, the effects of the entrainment of ambient air, sustained particle entrainment at the bed and stratification of suspended solids are secondary to the coupled processes of flow propagation under self-weight induced collapse and particle fallout from the driving, turbulent suspension. The relative importance of topography can be additionally assessed in the geometric measure $\lambda \equiv A/L^2$, which represents the azimuthal distribution of the deposit over area A with an overall, lateral runout distance L . In general, the axisymmetric model introduced here applies only to regionally widespread and landscape-mantling deposits for which λ is close to unity. At its upper limit, λ is equal to π in the case of a deposit that is completely radially widespread and axisymmetrically distributed about a vent. Values of λ much less than unity, on the other hand, are exhibited by many types of small-volume flows, including known densely concentrated, pyroclastic gravity currents, that are laterally confined and channelized by existing topography [Calder et al., 1999]. In such cases, independent evidence of dilute-flow behavior would be required before usefully applying the model invoked here. Other than these general constraints, the model relies on no freely adjustable parameters. The analysis thus provides a simple, yet potentially powerful tool with which one can consider the ‘order-of-magnitude’ dynamics of the regional transport of suspended material by a cataclysmic, topographically unconfined, gravity-driven flow.

[16] Among the potentially useful results of the analysis are diagnostic relationships between characteristic scales of duration and radial distance of flow runout as well as area of deposit inundation to the initial total volume, concentration and fall speed of individual particles in the driving suspension. These relationships are given in Table 2. The validity of the analysis has been experimentally established for laboratory flows with solids concentrations of up to about 30 per cent by volume [Dade and Huppert, 1994, 1995]. This concentration level is thus taken as an operationally defined upper limit to the dilute condition required of the model. A lower limit to solids concentration is simply that level required for a flow to be relatively denser than the ambient. These constraints aside, an application of the analysis does not require the assignment of a value of initial solids concentration a priori, but rather infers this value from characteristics of a regionally widespread deposit that mantles relatively flat terrain. Such interpretations yield meaningful estimates of the properties of the parent flows of analogous, submarine deposits known as turbidites [Dade and Huppert, 1994, 1995].

[17] Another interesting result of the analysis and experiments undertaken by *Dade and Huppert* [1995] is that, based on the distribution of a deposit alone, one cannot distinguish between a deposit emplaced by a parent flow with a source condition of constant flux from a deposit generated by the instantaneous release of a volume of dense suspension. The implication is that one is free to use whichever source condition is more convenient in interpreting deposit geometry. The analytical relationships considered here and given in Table 2 are for surge-like, turbulent gravity flows generated by the instantaneous release of a large volume of dense-particle suspension, with the understanding that for this scenario to be geologically reasonable the average volumetric eruptive flux Q must have been greater than the ratio of erupted volume versus an inferred time T of pyroclastic flow duration and deposit emplacement.

[18] The expressions given in Table 2 can be rearranged to yield estimates of the initial solids concentration C_0 , time of duration T and average flow speed U_{av} of the parent flow that generated an axisymmetric deposit of known sedimentary volume V_s , areal extent A and component particle size and density. One important simplification introduced here is that, when considering pyroclastic particles for which the characteristic grain size is greater than about 300 μm , the characteristic settling speed w_s in a low density gas is approximately given by $(g\gamma d)^{1/2}$, where γ and d are, respectively, the dimensionless, relative excess density and the characteristic diameter of individual particles. Upon substitution of this result and rearrangement of the equations given in Table 2, one obtains expressions for C_0 , T and U_{av} given by

$$C_0 \approx 8(\lambda V_s^3/A^4 d)^{1/2}, \quad (2)$$

$$T \approx (4A^2/\lambda g\gamma V_s)^{1/2}, \quad (3)$$

and

$$U_{av} \approx (g\gamma V_s/4A)^{1/2}. \quad (4)$$

Equations (2)–(4) reflect the assumption that the Froude number of a parent flow is unity. The time of duration T given in Table 2 and, with rearrangement, in equation (3), corresponds to the interval required for a flow to achieve about 98 percent of its overall extent. The approximation sign (\approx) is thus used to emphasize that these expressions yield notional estimates only.

[19] The characteristic values of the duration and speed of a parent flow introduced in equations (3) and (4) depend on the effective value of gravity, which is related to the relative excess density of individual particles γ . The estimate for the initial concentration of solids C_0 given by equation (2), however, is independent of particle and fluid densities. In this regard, the aspect ratio AR of an axisymmetric deposit is given by $\pi^{1/2} V_s/A^{3/2}$, and an expression equivalent to equation (2) for the initial concentration of solids is thus $C_0 \approx 8\{(\lambda AR/\pi)^3 L/d\}^{1/2}$. Alternatively, this result combined with equation (4) and the definition of the Froude number require that the average thickness of a parent flow be proportional to $A^{1/2}(d/L)^{1/2}/AR$. These quantitative links

between the properties of a deposit and its parent flow simply reflect the dimensional scalings that necessarily emerge from the physical model outlined above. The implication is that a deposit of finite extent and finite grain size that exhibits a very low-aspect ratio is necessarily associated with a relatively dilute and thick parent flow. For a class of deposits for which AR and d are constant, the inferred initial concentration of solids in the parent flow increases weakly with its overall extent of runout. This constraint simply reflects the volume of suspended ejecta required to drive a deposit-forming gravity current to greater distances. For a class of deposits of known radial extent and aspect ratio, the inferred initial value of C_0 decreases with increasing characteristic grain size.

[20] Once an estimate of the initial solids concentration C_0 of a deposit-forming flow is obtained, estimates of the initial volume V_0 and the nominal radius L_0 of an explosively emplaced, spheroidal eruption cloud are given simply by V_s/C_0 and $(3V_0/4\pi)^{1/3}$, respectively. The estimate L_0 provides a measure of the average height of the instantaneously emplaced eruption cloud before collapse (ignoring any thermal buoyancy effects), and of the radius of a blast zone immediately surrounding a volcanic vent. The simple flow model invoked here thus applies to gravity-current runout from explosive eruption clouds only for distances greater than L_0 .

[21] The product $g\rho V_s L_0$ corresponds to the mechanical energy required to elevate a mass of ejecta ρV_s to an average height L_0 , and is thus a measure of the explosive yield of the eruption. This estimate of yield does not include the amount of the energy required for the ascent of the ejecta from the subsurface magma chamber, or the thermal and acoustic energies released during an eruption. The amount of thermal energy released in an explosive eruption can be considerable, and even greater than the amounts of mechanical energy reckoned here [cf., *Pyle*, 1995]. An estimate of the mechanical yield nevertheless serves as a useful point of comparison with, say, the explosive yield of a nuclear device detonated at or just above the Earth's surface, and thus provides an alternative to the eruptive flux Q as a measure of eruption explosivity. Both measures are helpful for specialists and nonspecialists alike in evaluating the scale of the hazards associated with explosive volcanism.

4. A Quantitative Interpretation of Ignimbrites With Low-Aspect Ratio

[22] The LARIs described in Table 1 represent ancient pyroclastic deposits that exhibit axisymmetric and regionally widespread geometries for which AR is of order 10^{-4} or less and λ is of order unity. The Vulsini, Taupo, Koya and Tosu LARI's of intermediate volume have each been interpreted by the original investigators cited in Table 1 to comprise the product of a single, short-lived emplacement event, or "flow unit." The volumetrically larger deposits have been preliminarily interpreted by the cited investigators to represent individual flow units. They are included for the sake of comparison. All cases are subject to an analysis based on the model results outlined above. Accordingly, values of C_0 , T and U_{av} are inferred from the known characteristics of the respective deposits given in Table 1 using equations (2)–(4). In calculating each of these values,

it is assumed that the component particles in the ejecta of all eruptions have a characteristic diameter d of 1 mm and a density ρ of 1000 kg m^{-3} , and that the hot, interstitial gas had a density of 0.4 kg m^{-3} . The particle properties assigned here correspond approximately to the properties observed in recent surge deposits and ancient LARIs alike [e.g., *Druitt*, 1992]. The density of the interstitial gas corresponds to that of air at about 500°C . With these nominal values, the results of the model of *Dade and Huppert* [1995] constrain the initial concentration of solids in a source eruption cloud, on average, to be of the order of one per cent of the total cloud volume. As explained above, this value is independent of the choice of particle and fluid densities, and variation of the characteristic grain size d in the range 0.5–2 mm does not change the essence of this result. In the very largest LARI considered, the Rattlesnake Tuff, an inferred value of C_0 of several per cent is consistent with the significant conservation of heat that would have been required to result in the degree of welding observed in the deposit [*Streck and Grunder*, 1995].

[23] The inferred values of initial concentration of solids correspond to minimal eruptive fluxes of between 10^6 – $10^9 \text{ m}^3 \text{ s}^{-1}$ or, alternatively, to minimal, explosion-like yields of between 10^{11} J and 10^{20} J . The resulting eruption clouds virtually instantaneously attained maximal heights of up to about 10 km before any further lofting owing to thermal buoyancy. Such heights attained solely by inertial thrust correspond to vent-exit velocities of several hundred meters per second [cf. *Wilson et al.*, 1980; *Mastin*, 1995]. The collapse of the eruption clouds resulted in ground-hugging, pyroclastic gravity currents with average horizontal flow speeds in the range of 25 m s^{-1} to 250 m s^{-1} . The maximal time of duration of a LARI-forming flow is inferred to have been about 30 min for the radially wide-spread inundation of 10^4 km^2 .

[24] It is important to emphasize that the estimates given in Table 1 and summarized above represent notional conditions in the respective parent flows. Solids concentration and flow speed, for example, would have evolved during the course of each event. Also ignored here are the effects of a range of grain sizes in the driving suspension. However, in a more detailed analysis of the Taupo event in which the initial distribution of grain sizes in suspension was considered [*Dade and Huppert*, 1996], C_0 , U_{av} and T were estimated to be 0.003, 100 m s^{-1} and about 10 min, respectively. These values are comparable to the estimates for the Taupo event made here under somewhat different assumptions and given in Table 1. The key aspect of the eruption that renders the two analytical approaches comparable is that the eruptive flux of solids exceeded $10^7 \text{ m}^3 \text{ s}^{-1}$.

[25] The calculations summarized in Table 1 provide explicit values that are consistent with the notion that pumiceous ash-flow deposits with relatively low cross-sectional aspect ratio AR and relatively large plan aspect ratio λ are, in general, emplaced by highly expanded gravity currents derived from extremely explosive volcanic eruptions. In all cases, the inferred value of the ratio w_s/U_{av} is significantly less than unity, so that the condition imposed by equation (1) is satisfied for flows over terrain of relatively small regional slope. In all cases, the product ρC_0 exceeds the typical density of ambient air, and so is consistent with the existence of a relatively dense, ground-

hugging gravity current. The incorporation of more complicated dynamics that accommodate, say, the effects of density stratification, bedload transport of very large particles and topographic control of local, late-stage densely concentrated flows will result in refined estimates of the overall properties of the flows and their parent eruptions. The analysis developed here nevertheless yields physically consistent estimates of these properties for recent, turbulent surge deposits and ancient, large volume LARIs that sheds new light on emplacement dynamics and the nature of the ignimbrite deposits. In the next section, we explore one area of enquiry where this is the case.

5. The Products of Ignimbrite Eruptions Reconsidered

[26] An important conceptual development in the analysis of ancient pyroclastic deposits is the standard ignimbrite stratigraphy advanced by *Sparks et al.* [1973]. In this view, a vertical section of ignimbrite ideally exhibits a relatively thin basal layer of cross-bedded or fines-depleted and compositionally graded sediments (layer 1) overlain by a thick (10-cm to 10-m) layer of poorly sorted pumice, ash and lithics (layer 2). Although typically homogeneous, layer 2 can locally show crude planar laminations or inverse grading of particles by size in which a basal sublayer of relatively fine, dense lithics is overlain by a coarser and more pumiceous sublayer. Ideally capping the sequence is a thin layer of fine ash (layer 3). This simple picture has been modified and extended by various workers, but remains a keystone of textbook discussions of ignimbrite stratigraphy [e.g., *Francis*, 1993].

[27] The results of the analysis developed here contribute to the interpretation of LARI emplacement in terms of these deposit features. To summarize briefly, LARIs and surge deposits show similar degrees of mobility in terms of radial geometry, aspect ratio and ability to surmount topography. They show similar lateral trends in aerodynamic sorting and distribution of deposit. An important next step is to link ancient, low-aspect ratio ignimbrites and recent surge deposits with a quantitative physical model. This has been the aim here.

[28] In Figure 3, the area inundated by each of the low-aspect ratio deposits summarized in Table 1 is shown as a function of deposit volume adjusted for plan aspect. The solid line indicates the best fit regression that relates these two deposit properties using the relevant equation in Table 2, and for which the value of the product dC_0^2 is inferred to be 10^{-4} mm . Thus, for deposits in which the characteristic particle diameter is 1 mm, the initial volumetric concentration of solids in the parent flow C_0 is inferred to have been, on average, 10^{-2} for the events listed in Table 1 (and as was reported above). This result suggests that the parent flows of large volume, low-aspect ratio ignimbrites known only from the geologic record can be considered to be volumetrically and energetically “scaled up” pyroclastic surges. This view has important ramifications for the comparative interpretation of the internal stratigraphy of recent surge deposits and ancient LARIs.

[29] Regimes of bedform development under a turbulent flow are constrained by the shear stress imposed on the aggrading bed as well as the physical properties of the

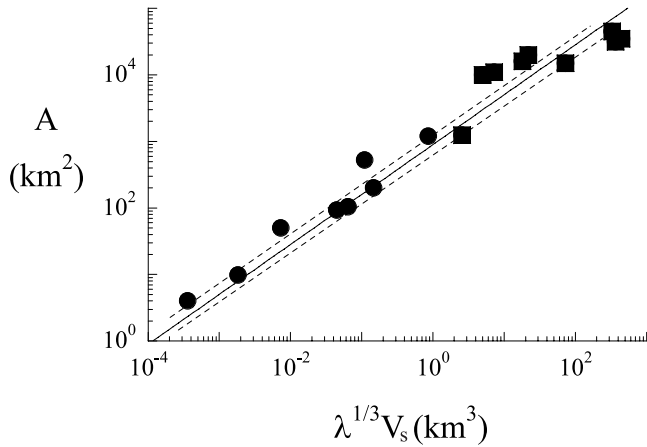


Figure 3. Area of inundation as a function of adjusted volume of solids for pyroclastic deposits of low-aspect and listed in Table 1. The filled circles indicate deposits emplaced by turbulent, pyroclastic surges of recent history. The squares indicate large-volume LARIs known only from the geologic record. The solid line indicates a nonlinear, least squares regression of the relevant equation in Table 2 with $F = 1$ and $w_s = (g\gamma d)^{1/2}$, which corresponds to $dC_0^2 = 10^{-4}$ mm ($R^2 = 0.8$). The dashed lines indicate similar calculations for $dC_0^2 = 0.5 \times 10^{-4}$ mm and 2×10^{-4} mm.

grains and fluid in transport [Allen, 1982; Middleton and Southard, 1984]. Shown in Figure 4, as a function of deposit volume, are notional estimates of the dimensionless bed shear stress $\Theta = fU_{av}^2/g\gamma d$ for the inferred, average speed U_{av} (equation (4)) of the parent flows of each of the deposits listed in Table 1, a drag coefficient f with a value of 0.01, and, as above, $d = 1$ mm and $\gamma = 2500$. Rendering shear stress dimensionless in this way allows a tentative analogy with subaqueous flows. The analogy is decidedly not one-to-one, and the issues pursued here are meant only to provide one possible perspective.

[30] In subaqueous settings, flows in which the value of Θ is of the order of unity or slightly less are characterized by low-to-moderate stage transport conditions which can give rise to undulatory, dune-like bedforms and internally cross-stratified deposits. Deposit-forming flows in which the value of Θ is much greater than unity, on the other hand, are characterized by intense, sheet-like flow of granular material newly arrived at the bed and the suppression of undulatory bedforms. Accordingly, this regime results in the emplacement of deposits with massive bedding, inverse grading and/or planar laminations depending on, among other things, the range of grain sizes present and the rate of particle fallout from suspension. In the terminology applied to analogous, submarine turbidites, upper-stage transport conditions should yield an ignimbrite stratigraphy which may be the subaerial analog to layers A and B in the turbiditic Bouma sequence, and moderate-to-low stage transport conditions should result in deposits which may be subaerial analogs to Bouma layer C [cf. Allen, 1982; Pickering et al., 1989]. In a flow that undergoes significant evolution of transport intensity over the course of its duration, spatial and temporal patterns of bedform development that span all conditions can result.

[31] Neither the values of Θ inferred for individual events nor the boundary of $\Theta \approx 1$ between upper- and lower-stage regimes shown in Figure 4 should be taken too literally. Figure 4 nevertheless indicates the possible range of dynamic conditions in turbulent, pyroclastic gravity currents, and hence indicates the possible range of internal stratigraphies in resulting layer 2 deposits. These differences need to be accommodated when considering the products of ignimbrite eruptions. Relatively small-volume surges of recent history are characterized by moderate-to-low stage transport conditions. The implication is that a deposit emplaced by such surges records a component of tractive transport that can result in undulatory bedforms and internal cross stratification. The degree to which such bedding features develop will depend on, among other things, the duration of the typically short-lived event, the degree of density stratification in the parent flow and the rate of fallout of suspended material [e.g., Lowe, 1988]. Examples include the deposits emplaced during the May 1980 eruption of Mount St. Helens and the 1982 eruption of El Chichón.

[32] With increasing magnitude of an eruption and its ensuing pyroclastic gravity current, the resulting LARI is increasingly likely to reflect fallout of suspended material coupled with intense, sheet-like flow of granular material newly arrived at the rapidly aggrading bed. Under such conditions, undulatory bedforms are suppressed, and relatively large clasts can be transported large distances in

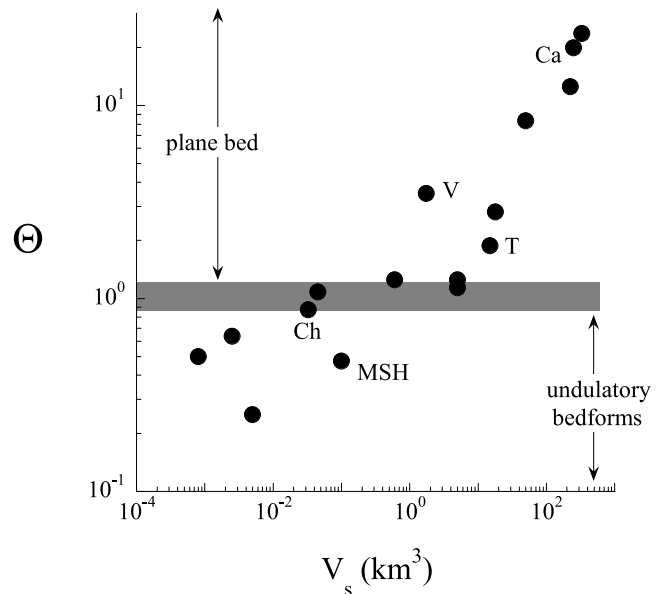


Figure 4. Inferred values of the dimensionless parameter Θ as a function of volume of solids in pyroclastic deposits of low-aspect. The filled circles indicate deposits emplaced by turbulent pyroclastic surges of recent history. The squares indicate large-volume LARIs known from the geologic record. Surges associated with the recent eruptions of Soufriere Hills Volcano, Montserrat (M), El Chichón (Ch) and Mount St Helens (MSH) as well as the ancient Taupo (T) and Campanian (Ca) ignimbrites are indicated for comparison. Proposed regimes of bed form occurrence are based on analogy with subaqueous flows.

bedload (the actual distance being constrained by the relative intensity and history of the waning parent flow). The deposit overall, moreover, will comprise predominantly shear-related features which could be mistaken for signatures of parent flows that are densely concentrated throughout, rather than only within the immediate vicinity of the bed. Such features can include (again depending on the range of grain sizes available and the rate of fallout of suspended particles) crude laminations, normally to-inverse grading of component particles by size and density, and massive, structureless beds. This is an important distinction from most, previous interpretations—in the perspective developed here, the densely concentrated, near-bed layer that controls LARI depositional structures is itself driven by and supplied sediment from an intensely turbulent, dilute, overlying parent flow of regional extent. As the parent flow decelerates in time and space owing to the loss of suspended material to deposition, features characteristic of low-to-moderate transport stages may develop. Examples of LARIs that exhibit massive structures and crude laminations include deposits with intermediate and extremely large volumes, such as the Taupo and Campanian ignimbrites.

6. Conclusions

[33] The emplacement of regionally widespread pyroclastic deposits involves the complex interaction of many physical processes on a wide range of scales. These processes include the physics of the parent eruptions themselves, the regional transport and deposition of multiphase ejecta, as well as the late-stage and local transport phenomena that affect the ultimate distribution and structure of a deposit. Assuming that explosive volcanic eruptions result in highly expanded and turbulent clouds of hot, yet relatively dense gas and ash, an analytical model for a radially spreading, suspension-driven gravity current can be used to infer the large-scale properties of the ensuing, ground-hugging flows that result in regionally widespread, pyroclastic deposits of low cross-sectional aspect ratio. A consistent picture emerges in which the initial volumetric concentration of solids in the ground-hugging flows that emanate from some explosive eruption clouds is of the order 10^{-2} or less, and these deposit-forming flows travel with average speeds in the range 25–250 m s^{-1} . These values imply that the flows are capable of surmounting substantial topographic obstacles and reaching their furthest lateral extent in a matter of minutes. This is consistent with direct observations of recent, small-magnitude events and the distribution and the inferred travel paths of ancient, large-volume deposits. The diagnostic expressions given here which relate properties of deposit properties to the dynamics of the parent flows complement more detailed, numerical treatments of ash flows.

[34] The perspective promoted here recognizes that the principal hazards to life associated with the parent flows of low-aspect ratio ignimbrites are not impact and burial by a densely concentrated avalanche of ejecta, but rather asphyxiation and burns incurred in a hot, dusty gas, the impact of large individual particles in saltation transport, and the widespread structural damage brought on by particle-laden, hurricane-force winds. In the event, there is virtually no time to respond to an oncoming threat. Drawing on the

studies by Fisher [1990] and Calder *et al.* [1999], among others, secondary, avalanche-like hazards can exist in rugged terrain where newly deposited material that is partially fluidized by exolving gases may drain into low-lying areas.

[35] A trend of increasing average flow speed with the magnitude of an eruptive event suggests that the primary depositional structures of low-aspect ratio ignimbrites can vary from that associated with predominantly moderate-to-low stage transport conditions in small-magnitude surges of recent history, to structures associated with predominantly upper-stage transport conditions in the parent flows of large volume deposits known only in the geologic record. Thus, details of the internal stratigraphy of a low-aspect ratio ignimbrite are likely to reflect the scale of the parent eruption and ensuing pyroclastic gravity current. A comparison of small-scale depositional structures in recent, small-volume surge deposits and ancient, large-volume LARIs that does not consider this potential difference in large-scale dynamics and evolution of the parent flows should be viewed with caution.

[36] A key issue which remains to be addressed is the delineation of conditions that determine whether a deposit-forming pyroclastic flow is highly expanded, as is proposed for the cases considered here, or is densely concentrated and avalanche-like, as for some of the pumiceous pyroclastic flows associated with the 1912 eruption of Katmai. Wilson *et al.* [1995] offer some insightful remarks regarding the potential significance of caldera collapse during very large, ignimbrite-forming eruptions. Those cases for which information is available indicate that relatively low-aspect deposits are associated with brief, unhindered and explosive eruptions from single, well-defined vents. Ignimbrites with relatively high aspect ratios, on the other hand, appear to be associated with syn-eruptive caldera collapse and the development of multiple, long-lived vents. The continued study of pyroclastic deposits of high and low-aspect alike, in conjunction with dynamically consistent models of their emplacement on regional and local scales, will contribute to our understanding of this important distinction.

[37] **Acknowledgments.** H. E. Huppert, P. Kokelaar, L. G. Maslin, D. M. Pyle, S. Self, R. S. J. Sparks, G. Valentine, and A. Woods made helpful comments on earlier versions of the text. The Natural Environment Research Council (UK) provided financial support. E. Dade provided just about everything else.

References

- Allen, J. R. L., *Sedimentary Structures, Developments in Sedimentology* 30, Elsevier Sci., New York, 1982.
- Aramaki, S., and Y. Ui, The Aira and Ata pyroclastic flows and related caldera and depressions in Southern Kyushu, Japan, *Bull. Volcanol.*, 29, 29–47, 1966.
- Branney, M. J., and P. Kokelaar, A reappraisal of ignimbrite emplacement: Progressive aggradation and changes from particulate to non-particulate flow during emplacement of high-grade ignimbrite, *Bull. Volcanol.*, 54, 504–520, 1992.
- Bursik, M. I., and A. W. Woods, The dynamics and thermodynamics of large ash flows, *Bull. Volcanol.*, 58, 175–193, 1996.
- Calder, E. S., et al., Mobility of pyroclastic flows and surges at the Soufriere Hills Volcano, Montserrat, *Geophys. Res. Lett.*, 26, 537–540, 1999.
- Dade, W. B., and H. E. Huppert, Predicting the geometry of deep-sea turbidites, *Geology*, 22, 645–648, 1994.
- Dade, W. B., and H. E. Huppert, Runout and fine-sediment deposits of axisymmetric turbidity currents, *J. Geophys. Res.*, 100, 18,597–18,609, 1995.

- Dade, W. B., and H. E. Huppert, Emplacement of the Taupo ignimbrite by a dilute turbulent flow, *Nature*, 381, 509–510, 1996.
- Dade, W., and B. Huppert, Long runout rockfalls, *Geology*, 26, 83–86, 1998.
- Druitt, T. H., Emplacement of the 18 May 1980 lateral blast deposit ENE of Mount St. Helens, Washington, *Bull. Volcanol.*, 54, 554–572, 1992.
- Druitt, T. H., Pyroclastic density currents, in *The Physics of Explosive Volcanic Eruptions*, edited by J. S. Gilbert and R. S. J. Sparks, Geol. Soc. Spec. Publ., 145, 145–182, 1998.
- Fisher, R. V., Mechanisms of deposition from pyroclastic flows, *Am. J. Sci.*, 264, 350–363, 1966.
- Fisher, R. V., Transport and deposition of a pyroclastic surge across and area of high relief: The 18 May 1980 eruption of Mount St. Helens, Washington, *Geol. Soc. Am. Bull.*, 102, 1038–1054, 1990.
- Fisher, R. V., G. Orsi, M. Ort, and G. Heiken, Mobility of a large-volume pyroclastic flow—Emplacement of the Campanian ignimbrite, Italy, *J. Volcanol. Geotherm. Res.*, 56, 205–220, 1993.
- Francis, P., *Volcanoes*, 443 pp., Oxford Univ. Press, New York, 1993.
- Gilbert, J. S., and R. S. J. Sparks, Future research directions on the physics of explosive volcanic eruptions, in *The Physics of Explosive Volcanic Eruptions*, edited by J. S. Gilbert and R. S. J. Sparks, Geol. Soc. Spec. Publ., 145, 1–7, 1998.
- Hayashi, J. N., and S. Self, A comparison of pyroclastic flow and debris avalanche mobility, *J. Geophys. Res.*, 97, 9063–9071, 1992.
- Iverson, R. M., S. P. Schilling, and J. W. Vallance, Objective delineation of lahar-inundation hazard zones, *Geol. Soc. Am. Bull.*, 110, 972–984, 1998.
- Koch, A. J., and H. McLean, Pleistocene tephra and ash-flow deposits in the volcanic highlands of Guatemala, *Geol. Soc. Am. Bull.*, 86, 529–541, 1975.
- Lowe, D. R., Suspended fallout rate as an independent variable in the analysis of current structures, *Sedimentology*, 35, 765–776, 1988.
- Mastin, L. G., Thermodynamics of gas and stream-blast eruptions, *Bull. Volcanol.*, 57, 85–98, 1995.
- McKee, C. O., R. W. Johnson, P. L. Lowenstein, S. J. Riley, R. J. Blong, P. De Saino Ours, and B. Talai, Rabaul Caldera, Papua New Guinea: Volcanic hazards, surveillance, and eruption contingency planning, *J. Volcanol. Geotherm. Res.*, 23, 195–237, 1985.
- Middleton, G. V., and J. B. Southard, *Mechanics of Sediment Movement*, 401 pp., Soc. of Econ. Paleontol. and Mineral., Tulsa, Okla., 1984.
- Moore, J. G., Base surges in recent volcanic eruptions, *Bull. Volcanol.*, 30, 337–363, 1967.
- Moore, J. G., and T. W. Sisson, Deposits and effects of the May 18 pyroclastic surge, *U. S. Geol. Surv. Prof. Pap.*, 1250, 421–438, 1983.
- Pickering, K. T., R. N. Hiscott, and F. J. Hein, *Deep Marine Environments*, 416 pp., Chapman and Hall, New York, 1989.
- Pyle, D. M., Mass and energy budgets of explosive volcanic eruptions, *Geophys. Res. Lett.*, 22, 563–566, 1995.
- Sigurdsson, H., S. N. Carey, and J. M. Espindola, The 1982 eruptions of El Chichón volcano, Mexico: Stratigraphy of pyroclastic deposits, *J. Volcanol. Geotherm. Res.*, 23, 11–37, 1987a.
- Sigurdsson, H., S. N. Carey, and R. V. Fisher, The 1982 eruptions of El Chichón volcano, Mexico (3): Physical properties of pyroclastic surges, *Bull. Volcanol.*, 49, 467–488, 1987b.
- Simkin, T., and L. Seibert, *Volcanoes of the World*, 349 pp., Geoscience, Tucson, Ariz., 1994.
- Simpson, J. E., *Gravity Currents*, 244 pp., John Wiley, New York, 1987.
- Sparks, R. S. J., Stratigraphy and geology of the ignimbrites of Vulcini Volcano, Central Italy, *Geol. Rundsch.*, 64, 497–523, 1975.
- Sparks, R. S. J., and L. Wilson, A model for the formation of ignimbrite by gravitational column collapse, *J. Geol. Soc. London*, 132, 441–451, 1976.
- Sparks, R. S. J., S. Self, and G. P. L. Walker, Products of ignimbrite eruptions, *Geology*, 1, 115–118, 1973.
- Sparks, R. S. J., L. Wilson, and G. Hulme, Theoretical modelling of the generation, movement, and emplacement of pyroclastic flows by column collapse, *J. Geophys. Res.*, 83, 1727–1739, 1978.
- Streck, M. J., and A. L. Grunder, Crystallization and welding variations in a widespread ignimbrite sheet; the Rattlesnake Tuff, eastern Oregon, USA, *Bull. Volcanol.*, 57, 151–169, 1995.
- Susuki-Kamata, K., and H. Kamata, The proximal facies of the Tosu pyroclastic-flow deposit erupted from Aso caldera, Japan, *Bull. Volcanol.*, 52, 325–333, 1990.
- Torres, R. C., S. Self, and M. L. Martinez, Secondary pyroclastic flows from the June 15, 1991 ignimbrite of Mount Pinatubo, in *Fire and Mud: Eruptions and Lahars of Mount Pinatubo, Philippines*, edited by C. G. Newhall and R. S. Punongbayan, 1126 pp., Univ. of Washington Press, Seattle, Wash., 1997.
- Valentine, G. A., Stratified flow in pyroclastic surges, *Bull. Volcanol.*, 49, 616–630, 1987.
- Valentine, G. A., and R. V. Fisher, Glowing avalanches: New Research on volcanic density currents, *Science*, 259, 1130–1131, 1993.
- Valentine, G. A., and K. H. Wohletz, Numerical models of plinian eruption columns and pyroclastic flows, *J. Geophys. Res.*, 94, 1867–1887, 1989.
- Walker, G. P. L., Ignimbrite types and ignimbrite problems, *J. Volcanol. Geotherm. Res.*, 17, 65–88, 1983.
- Walker, G. P. L., R. F. Heming, and C. J. N. Wilson, Low-aspect ratio ignimbrites, *Nature*, 283, 286–287, 1980.
- Waters, A. C., and R. V. Fisher, Base surges and their deposits: Capelinhos and Taal Volcanoes, *J. Geophys. Res.*, 76, 5596–5614, 1971.
- Wilson, C. J. N., The role of fluidization in the emplacement of pyroclastic flows: An experimental approach, *J. Volcanol. Geotherm. Res.*, 8, 231–249, 1980a.
- Wilson, C. J. N., The Taupo eruption, New Zealand, II, The Taupo Ignimbrite, *Philos. Trans. R. Soc. London, Ser. A*, 314, 229–310, 1985.
- Wilson, C. J. N., W. B. Dade, and H. E. Huppert, Scientific correspondence regarding Dade and Huppert [1996], *Nature*, 385, 306–308, 1997.
- Wilson, C. J. N., B. F. Houghton, P. J. J. Kamp, and M. O. McWilliams, An exceptionally widespread ignimbrite with implications for pyroclastic flow emplacement, *Nature*, 378, 605–607, 1995.
- Wilson, L., Relationships between pressure, volatile content and ejecta velocity in three types of volcanic explosion, *J. Volcanol. Geotherm. Res.*, 8, 297–313, 1980b.
- Woods, A. W., Observations and models of volcanic eruption columns, in *The Physics of Explosive Volcanic Eruptions*, edited by J. S. Gilbert and R. S. J. Sparks, Geol. Soc. Spec. Publ., 145, 91–114, 1998.

W. B. Dade, Department of Earth Sciences, Dartmouth College, Hanover, NH 03755, USA. (Brian.Dade@dartmouth.edu)